Prediction Models for Mechanical Properties of Cement-Bound Aggregate with Waste Rubber

Zvonarić, Matija; Benšić, Mirta; Barišić, Ivana; Dokšanović, Tihomir

Download date / Datum preuzimanja: **2025-03-14**

Article

Prediction Models for Mechanical Properties of Cement-Bound Aggregate with Waste Rubber

Matija Zvonarić [1], Mirta Benšić [2], Ivana Barišić [1,*] and Tihomir Dokšanović [1]

1 Faculty of Civil Engineering and Architecture Osijek, Josip Juraj Strossmayer University of Osijek, 31000 Osijek, Croatia; mzvonaric@gfos.hr (M.Z.); tdoksanovic@gfos.hr (T.D.)
2 Department of Mathematics, Josip Juraj Strossmayer University of Osijek, 31000 Osijek, Croatia; mirta@mathos.hr
* Correspondence: ivana@gfos.hr

Abstract: The high stiffness of cement-bound aggregate (CBA) is recognized as its main drawback. The stiffness is described by the modulus of elasticity, which is difficult to determine precisely in CBA. Incorporating rubber in these mixtures reduces their stiffness, but mathematical models of the influence of rubber on the mechanical characteristics have not previously been defined. The scope of this research was to define a prediction model for the compressive strength (f_c), dynamic modulus of elasticity (E_{dyn}) and static modulus of elasticity (E_{st}) based on the measured ultrasonic pulse velocity as a non-destructive test method. The difference between these two modules is based on the measurement method. Within this research, the cement and waste rubber content were varied, and the mechanical properties were determined for three curing periods. The E_{dyn} was measured using the ultrasonic pulse velocity (UPV), while the E_{st} was determined using three-dimensional digital image correlation (3D DIC). The influence of the amount of cement and rubber and the curing period on the UPV was determined. The development of prediction models for estimating the f_c and E_{st} of CBA modified with waste rubber based on the non-destructive test results is highlighted as the most significant contribution of this work. The curing period was statistically significant for the prediction of the E_{st}, which points to the development of CBA elastic properties through different stages during the cement-hydration process. By contrast, the curing period was not statistically significant when estimating the f_c, resulting in a simplified, practical and usable prediction model.

Keywords: prediction models; cement-bound aggregate; waste rubber; compressive strength; modulus of elasticity; ultrasonic pulse velocity; non-destructive testing

1. Introduction

In semi-flexible pavements, cement-bound aggregate (CBA) is used as a bearing layer. This layer provides improved bearing capacity and freeze—thaw resistance while presenting an even surface for installing asphalt layers. Despite all the benefits, these materials are prone to cracking due to cement hydration and the expansion of these cracks under the influence of repeated traffic loads [1]. Recently, waste rubber has been used in this material to release internal stresses and reduce the occurrence of cracks. The quality of this material is primarily described by its compressive strength. The compressive strength of CBA is usually tested after 7 and 28 days [2], but it is often measured after 90, 180 and 360 curing days for CBA modified with materials possessing postponed pozzolanic activity. The strength is significantly lower than that of conventional concrete, and satisfactory 7-day compressive strength ranges from 2.1 to 2.8 MPa [3,4]. Determining the compressive strength implies measuring the breaking force of a sample exposed to a uniaxial compressive load. The destruction of a sample is an acceptable way of testing laboratory-prepared samples when a sufficient number of samples can be produced. However, when evaluating the material incorporated in a pavement, there is a limited number of cored specimens. Preserving the

sample for many test procedures is very useful in this case. Additionally, conducting a field evaluation of the inbuilt bearing layer using non-destructive testing is preferable.

The other important characteristic of cement-bound aggregate is its elasticity modulus (E). The dynamic (E_{dyn}) and static (E_{st}) moduli of elasticity can be measured within cement-based materials [5]. The E_{st} is determined from the linear relationship of the stresses and strains during the compression strength test. An obstacle in determining the static modulus of elasticity is the rough surface of this material [6], because the procedure entails the precise measurement of microscopic vertical displacements of points on the sample derivatives during the change in compression force. In addition to the difficulty of ensuring precise measurements, this is also a destructive method. At the same time, the static modulus of elasticity is significantly lower than the dynamic modulus [6].

On the other hand, the dynamic modulus of elasticity is usually measured using the ultrasonic pulse velocity. This is a non-destructive method, usually used in concrete testing, after which the sample is ready for further testing, and it can be applied to various materials. Ultrasonic pulses are pulses with frequencies over 20 Hz. There are several conventional ultrasonic testing methods, such as the pulse-echo ultrasonic, pitch-catch ultrasonic, immersion-based ultrasonic, air-coupled ultrasonic, oblique incidence, phase array ultrasonic and laser-ultrasonics and non-contact laser-ultrasonic techniques [7]. The choice of method depends on the tested material, the size of the specimen and external conditions. As mentioned above, cement hydration is a time-dependent process, so the passage of time significantly affects the development of the material stiffness. Guotang et al. [8] explain three typical stages of UPV development during the first 55 h of cement-stabilized aggregate microstructure formation. In the first stage, the UPV is stable at low values, followed by the second stage, where, due to cement hydration, the UPV rapidly increases. In the third stage, the UPV gradually becomes stable due to a rigid and stable matrix.

These methods apply to all materials used in road construction, starting from the stabilized soil through bearing layers to asphalt materials. Raavi and Tripura [9] developed prediction models for compressive and indirect tensile strength estimation of unstabilized and stabilized rammed earth based on UPV measurement. The authors also encourage using UPV measurement as an effective strength-estimation method. Furthermore, in [10], the authors emphasize that to develop prediction models, it is necessary to increase the number of UPV measurements in each direction (x, y, z) to four to increase the precision of the results. In addition, the importance of not carrying out measurements at the same point on the sample is emphasized. A prediction model for shear modulus estimation was developed in [11] by applying this method to cement-stabilized clays. The UPV proved helpful in multifunctional analysis, which predicts the compressive strength and rebound value [11]. Furthermore, this non-destructive method achieved reliable results in evaluating cement-bound aggregate. Barišić et al. [12] observed a strong relationship between the UPV and the compressive- and indirect-tensile-strength values and emphasized polynomial and exponential laws as the most appropriate to describe the relationship between strength and UPV. They also defined a range of UPVs in which CBA achieves satisfactory characteristics, which is helpful when making decisions during an examination. This paper develops models for steel-slag-stabilized mixtures for three different curing ages: 7, 28 and 90 days. Liu et al. observed a difference between compression and tension modulus and developed a power function decay model for these two parameters [13]. According to Mandal et al. [14], the UPV can be used to estimate the mechanical properties of most cement-stabilized materials, except cement-stabilized clay, which behaves differently from other stabilized materials. This paper presents strong correlations in the developed models between the flexural strength and the constrained modulus and the flexural modulus and the constrained modulus based on 7-day-old specimens. These parameters are commonly tested for the evaluation of soil behavior. In addition to CBA, roller-compacted concrete (RCC) is also used in pavement construction. Regarding its mechanical properties, this material occupies a place between CBA and concrete. Prediction models have also been

developed for such materials, which predict the compressive strength based on the rebound number and the UPV [15]. The relationship between the rebound number and the compressive strength is established by the power law, while the relationship between the UPV and compressive strength is established by the exponential law. Additionally, the authors developed a logarithmic relationship between the dynamic modulus of the elasticity and the compressive strength. Furthermore, Rao et al. [16] developed an equation for estimating the E_{dyn} of the RCC based on the fly ash content, UPV and curing period, which agrees with experimental tests. The RCC in these research works is combined with crumb rubber, nano-silica and fly ash, making UPV a universal tool for model development in different materials. The UPV mainly served as a compressive-strength-prediction tool in the research on stabilized granular materials and no research deals with the issue of the static modulus of elasticity. Furthermore, all the models of CBA developed are nonlinear. There is a consensus on the utility of using the UPV technique when evaluating the mechanical characteristics of coherent [9–11,17] and incoherent materials [18]. The reliability of all the developed models is based on the coefficient of determination, which is not a reliable parameter for evaluating nonlinear models in the sphere of statistical inference. Therefore, the need for a more detailed statistical data analysis in this area is emphasized.

The non-destructive nature of UPV measurement also applies to asphalt mixtures. Norambuena-Contreras et al. [19] state that the dynamic modulus measured by the UPV can replace the low-frequency standard dynamic test. They also emphasize this method as cheaper, faster and easier to implement. In determining the E_{dyn} of asphalt mixtures by UPV, Majhi et al. [20] concluded that more reliable modulus values are obtained by considering the bulk density rather than the geometric density of asphalt specimens. The testing of the moisture sensitivity of asphalt mixtures using the UPV in [21] resulted in a linear equation between the seismic modulus and the UPV with a good coefficient of determination. Using this model, the moisture susceptibility of asphalt specimens can be predicted.

In addition to the desire for non-destructive testing methods, the trend of the circular economy has also been expressed in recent times. There are increasing numbers of applications of different waste materials in composite materials used in construction. Some of these are used as aggregates, while those with pronounced pozzolanic properties are used as binders. For example, Jackowski et al. [22] investigated the possibility of using different additives to cement and different fibers in the production of concrete bricks, while Ramadani et al. [23] investigated the possibility of using glass powder in combination with waste rubber in concrete. Rubber has also showed potential in increasing the resistance of concrete structures to the impact of earthquakes [24]. Guided by the desire to preserve the environment, rubber was used as a waste material in this work, since, due to its pronounced elastic properties, it can affect the reduction in the high stiffness of cement-stabilized aggregates and, as a waste material, it is very easily available on the market, considering the large consumption of tires. In addition, in most countries in Europe, the collection and processing of tires is very well organized [25]. Furthermore, the possibilities of using waste rubber in road construction is highlighted [24,26]. However, prior to waste rubber's incorporation in pavement materials, it has to pass through a certain separation process, in which steel fibers are separated from the rubber. These steel fibers are applied as reinforcements in concrete [27].

The aim of this research is to develop reliable prediction models for f_c and E_{st} estimation based on the measured UPV of CBA modified with waste rubber. Such a model would ensure a simple, fast, non-destructive approach to characterizing CBA by adding waste rubber. Furthermore, based on the literature review, it is concluded that none of the prediction models developed to date consider both the UPV and the length of the curing regimes of specimens for the prediction of mechanical properties, which would greatly facilitate the application of such models. Furthermore, a complete lack of prediction models for estimating the static modulus of elasticity was observed. Considering the difficulty

of precisely determining this parameter, such a model would contribute significantly to this field.

2. Materials and Methods

Within this research, 15 cement-stabilized mixtures were tested. The materials used were natural river sand and gravel, waste granulated rubber, Portland cement of grade 32.5R (CEM II B/M (P-S) 32.5R) as a binder and the optimal amount of water determined according to standard [28]. The density of used materials is presented in Table 1, while the physical and mechanical properties of used binder are presented in Table 2.

Table 1. Densities of used material.

Aggregate	Sand		Gravel		Rubber	Cement
Size	0–2 mm	0–4 mm	4–8 mm	8–16 mm	0–0.5 mm	
Density (g/cm^3)	2.86	2.96	2.63	2.70	1.12	2.92

Table 2. Physical and chemical properties of cement.

Physical Properties		Chemical Properties	
Start of binding (min)	200	SO$_3$ (%)	3.2
Volume stability acc. to Le Chatelier (mm)	0.4	Cl (%)	0.009
Pressure strength after 2 days (MPa)	16		
Pressure strength after 28 days (MPa)	42		

The granulometric composition of the aggregates was determined using the European standard EN 933-1 [29] and is presented in Figure 1. The composition of the mixture shown in Figure 1 is tailored to the inclusion of rubber as per the flexibility allowed in the fifth category of the EN 14227-1 [30]. Cement was used as a binder in proportions of 3%, 5% and 7% of the aggregate mass. Due to their similar granulometric curves, fine-granulated rubber (0–0.5 mm) derived from end-of-life (ELT) car and truck tires was used as a volume replacement for sand in amounts of 10%, 20%, 30% and 40%. The detailed composition of the tested CBA mixtures is presented in Table 3. The rubber content is defined according to previous results, indicating 60% replacement, causing extremely high strength loss [31,32].
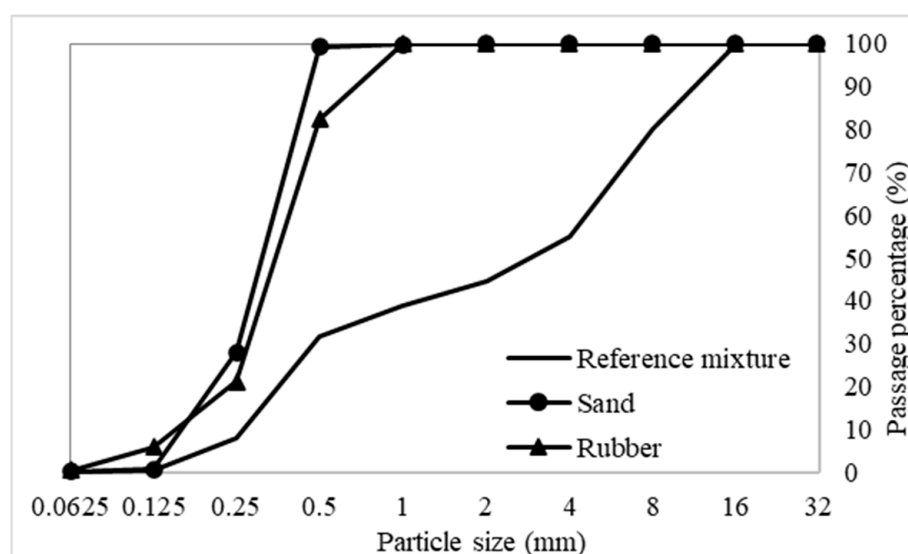

Figure 1. Granulometric composition.

Table 3. CBA mixture composition.

Mixture	Cement (%)	Sand (%)	Rubber (%)
C3R0		100	0
C3R10		90	10
C3R20	3	80	20
C3R30		70	30
C3R40		60	40
C5R0		100	0
C5R10		90	10
C5R20	5	80	20
C5R30		70	30
C5R40		60	40
C7R0		100	0
C7R10		90	10
C7R20	7	80	20
C7R30		70	30
C7R40		60	40

Rubber replacing the fine fraction complies with several other research papers [33–38]. Each rubber proportion was added to each cement amount, resulting in 12 rubberized mixtures. Three standard cylindrical specimens measuring Ø100 mm and with heights of 120 mm of each mixture were compacted by a vibrating hammer according to the procedure prescribed in EN 13286-51 [39].

The specimens were produced in order to test their compressive strength and determine their static (E_{st}) and dynamic (E_{dyn}) moduli of elasticity. The modulus of elasticity is the slope of a material's stress—strain curve with its elastic region. Before destructive testing, the non-destructive method for determining E_{dyn} was employed according to standard EN 12504-4 [40]. This method is carried out on specimens of known dimensions and density, with two transducers applied to opposite bases of cylindrical specimens, emitting ultrasonic waves and measuring the duration of their passage, which is used to calculate the E_{dyn}. Poisson's coefficient is needed for the calculation, for which the value 0.25 was adopted in this research as a typical value for CBA. Poisson's ratio usually ranges from 0.15 to 0.30 for cement-stabilized materials; the value of 0.25 was adopted in previous papers [41,42]. In addition, to neutralize the imperfect contact between the transducer and the rough specimen surface, a gel was applied. The procedure for determining the dimensions and mass of the specimen and the apparatus required for the UPV test are shown in Figure 2.

The measurement of E_{st} was carried out during the compressive strength test. The test was carried out according to EN 13286-43 [43] from the stress-and-strain relationship. Due to the inaccuracies in using LVDT for strain measurement, caused by the setting of the sample and the breakage of aggregates during the test, such results may be unreliable [6]. Therefore, in this research, a 3D DIC method was used to monitor the displacement of the characteristic points of the specimens. This is an optical non-contact method for monitoring the changes on the observed surface, in this case, vertical displacements. More details on the 3D DIC method used in this research and its applicability are presented in [44]. The procedure for E_{st} testing is shown in Figure 3. Testing of the compressive strength was carried out according to EN 13286-41 [45], exposing the specimen to a compressive load with the input force such that the fracture of the specimen occurred between the 30th and 120th second from the commencement of the load; specific experience is needed to conduct this test. The compressive strength was calculated from the peak force, i.e., the force at which the fracture occurred in the area on which the load was applied.
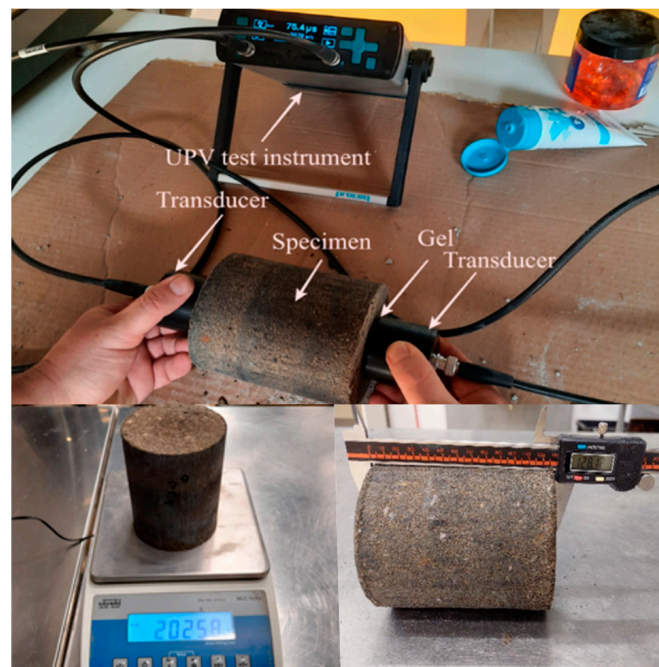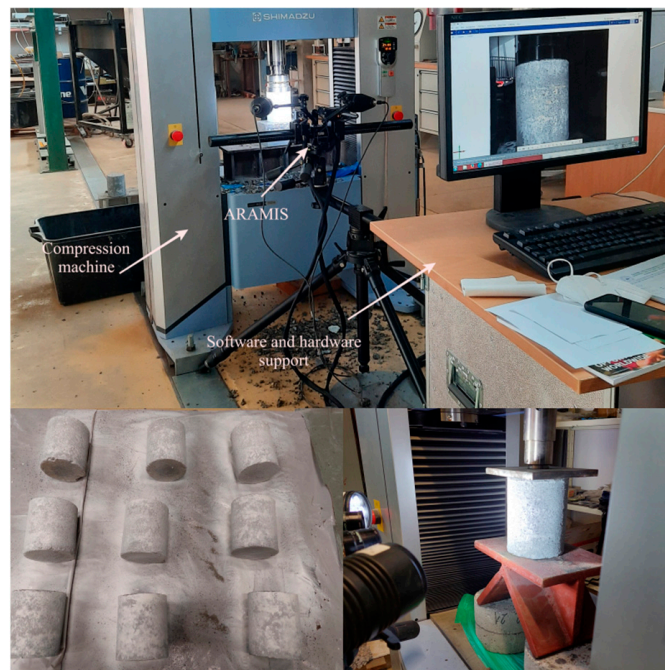
Figure 2. UPV testing.

Figure 3. The f_c and E_{st} testing.

3. Results

The results obtained for the dynamic modulus of elasticity (E_{dyn}), compressive strength (f_c) and static modulus of elasticity (E_{st}) measurements are shown in Table 4. The presented results were calculated as the average value of the three tested specimens for each mixture and curing period. Values that deviated by over 20% from each other were discarded according to the standard EN 14227-1 [30]. The table contains the results of the mechanical characteristics for the curing periods, 7, 28 and 90 days, and express the standard deviation (St.dev.). The mixtures were divided into groups (columns) according to the amount of rubber and, additionally, the results were divided according to the proportion of cement in the mixture. For example, the third, fourth and fifth columns in the table show the

results of mixtures with 0% rubber and 3%, 5% and 7% cement, respectively. From the plotted results (Table 4), it can be concluded that an increase in strength occurs with an increase in cement and in the duration of the curing period. The highest strength values were reached for the 90-day curing period and with 7% cement for each rubber content. On the other hand, increasing the amount of rubber in the mixture causes a decrease in the compressive strength. An increase in the E_{dyn} and E_{st} accompanies the increase in strength. The decrease in E_{din} and UPV with a decrease in f_c due to rubber incorporation complies with the findings in [16]. The authors of that paper state that a decrease in UPV is correlated with a decrease in compressive strength due to the incorporation of fly ash instead of cement, which has less early-age pozzolanic activity. In this case, the rubber is the reason for the compressive strength decrease. Observing the modulus values, one can conclude that there is no rapid modulus-growth phase, as stated in [8], because of the use of rapid hardening cement. The rapid growth in the strength and modulus occurred in the first seven days of the specimen curing. The same can be concluded from Figure 4, which shows the development of the UPV over time for the mixture with the highest cement content. These mixtures are shown because they are expected to have the most significant influence on the development of cement stiffness. It can be seen in Figure 4 that the difference between the UPV for 7 and 28 days increases with the amount of rubber because the hydration slows down due to the reaction of the Zn from the rubber with C3S [46]. However, for mixtures with up to 20% rubber, the UPV increases almost linearly until the 90th day of curing. It is impossible to determine the phase of the UPV's rapid growth as it is detected in rubberized mortars, i.e., the rapid growth phase occurs in the first 7 days. At the same time, the amount of 20% rubber was shown to reduce the initial development of the stiffness of the mixture. In general, the use of 20% rubber as a sand replacement reduces the rate of stiffness development and linearizes the stiffness development over time. This means that there is no sudden development of strength and stiffness and, consequently, no sudden development of internal stresses. Furthermore, by observing the static modulus of elasticity, it can be concluded that for reference mixtures, the E_{st} values stagnate for longer curing periods, and that this is more pronounced with higher cement contents. On the other hand, with the incorporation of rubber, the E_{st} develops with age and it is more pronounced with mixtures with higher cement contents. Greater changes in mixtures with higher proportions of cement and rubber directly indicate the interaction of rubber and cement.

Table 4. Results of f_c (MPa), E_{dyn} (GPa) and E_{st} (GPa) for three curing periods (7, 28 and 90 days) and corresponding standard deviations for f_c, E_{dyn} and E_{st}.

|		R0			R10			R20			R30			R40		
		C3	C5	C7	C3	C5	C7	C3	C5	C7	C3	C5	C7	C3	C5	C7
7 days	f_c	1.73	4.11	6.82	1.31	3.54	6.04	0.94	2.20	3.69	0.60	1.56	2.84	0.51	1.32	1.66
	St. dev. (f_c)	0.07	0.37	0.16	0.07	0.22	0.30	0.07	0.07	0.13	0.02	0.07	0.03	0.01	0.04	0.02
	E_{dyn}	11.39	20.04	27.14	9.35	17.79	23.22	3.23	10.93	14.76	1.76	5.66	9.05	0.62	4.18	4.19
	St. dev. (E_{dyn})	0.07	0.94	0.80	0.27	0.57	0.66	0.28	0.89	0.74	0.05	0.26	0.60	0.01	0.17	0.12
	E_{st}	2.27	4.61	10.76	2.11	5.46	7.25	1.63	3.79	4.94	0.73	2.03	3.78	0.59	1.53	1.80
	St. dev. (E_{st})	0.03	0.37	0.50	0.16	0.38	0.17	0.03	0.22	0.26	0.06	0.13	0.00	0.03	0.08	0.10
28 days	f_c	2.69	6.45	8.89	2.07	3.99	7.81	1.15	3.01	4.36	0.85	1.94	3.32	0.59	1.51	1.09
	St. dev (f_c)	0.31	0.07	0.27	0.09	0.09	0.22	0.02	0.03	0.29	0.02	0.11	0.03	0.01	0.04	0.03
	E_{dyn}	15.64	27.05	31.33	11.90	20.43	28.10	6.72	13.88	18.67	4.58	8.59	12.31	1.80	6.43	4.24
	St. dev. (E_{dyn})	1.00	1.00	0.27	0.54	0.41	1.26	0.12	0.34	1.42	0.16	0.14	0.53	0.07	0.35	0.40
	E_{st}	3.46	10.03	11.96	3.27	6.18	8.61	2.51	4.31	5.51	1.76	3.24	3.59	0.91	2.55	2.73
	St. dev. (E_{st})	0.026	0.53	0.12	0.04	0.41	0.17	0.17	0.01	0.46	0.03	0.05	0.20	0.05	0.13	0.08
90 days	f_c	3.32	7.55	11.57	3.88	7.67	12.95	2.24	4.85	7.85	1.13	2.78	4.30	0.84	2.13	2.34
	St. dev. (f_c)	0.11	0.53	0.38	0.05	0.00	0.46	0.06	0.12	0.20	0.05	0.13	0.20	0.01	0.00	0.03
	E_{dyn}	18.77	25.70	31.59	24.23	27.60	31.29	15.50	18.89	26.14	7.19	12.94	15.95	2.26	8.01	6.70
	St. dev. (E_{dyn})	1.11	0.98	0.45	1.30	0.74	1.04	0.99	1.72	0.66	0.42	0.26	0.45	0.03	0.39	0.19
	E_{st}	4.66	9.54	12.69	5.26	11.42	13.42	5.80	8.48	12.92	3.06	4.72	5.96	0.92	3.07	3.27
	St. dev. (E_{st})	0.35	0.57	0.79	0.23	0.39	0.40	0.15	0.09	0.61	0.10	0.11	0.42	0.02	0.10	0.19
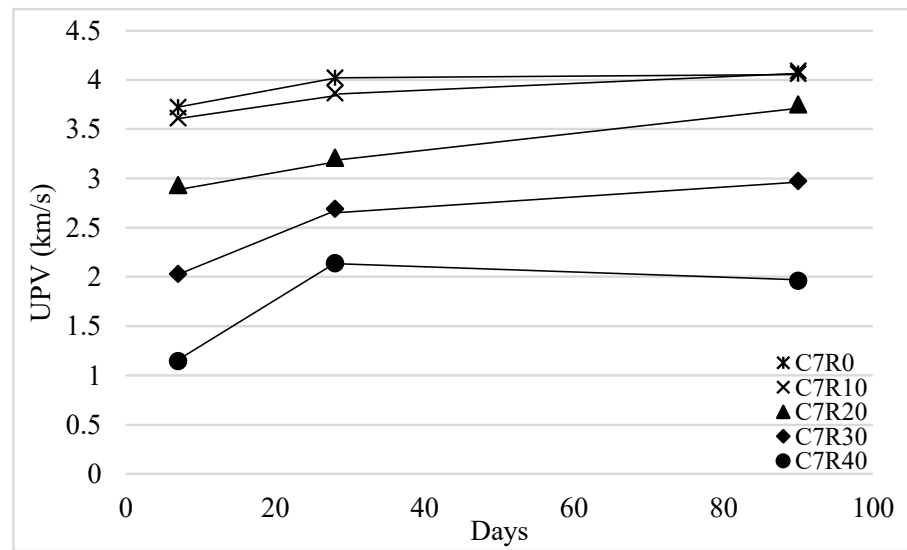
Figure 4. UPV development over time.

Furthermore, there is a strong linear correlation between these two moduli of the examined mixtures, with a coefficient of determination of $R^2 = 0.88$, as presented in Figure 5. There was inevitably a connection between these two material properties, which was expected, since these two parameters describe the same material property, its stiffness. The results are more homogeneous for lower elasticity modulus values, i.e., mixtures of lower strength and with a higher proportion of rubber. This is due to the more elastic behavior of these mixtures, the more uniform development of deformations during loading and, thus, the possibility of a more precise E_{st} determination. Considering that different methods are used to measure these two values and describe the same material characteristic, stiffness, their linear relationship is proof of the applicability of these two methods.
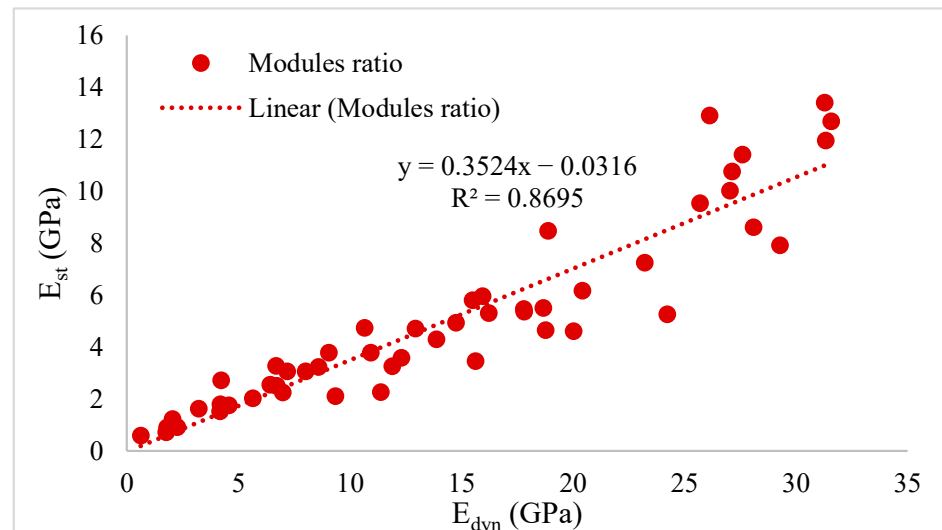

Figure 5. E_{dyn} and E_{st} relationship.

In this paper, we try to understand the relationship between the measured UPV and the mechanical characteristics to establish prediction models. Firstly, the impact of the amount of cement and rubber and the curing period on the UPV is analyzed. The UPV values for each mixture are presented in Figure 6a for 7 days, Figure 6b for 28 days and Figure 6c for 90 days. As shown in Figure 6, the ultrasonic pulse travels faster through mixtures with higher proportions of cement, resulting in a very rigid matrix, which is more

pronounced for shorter curing periods. That is, mixtures with higher proportions of cement have more cement paste, which has a significantly higher stiffness than other mixture constituents. In Figure 6c, one can see the decrease in the UPV for the C7R40 mixture, which is attributed to the large amount of fine particles of rubber and cement, resulting in the filling of all the pores and the grouping of the rubber in clusters that form an obstacle to the passage of ultrasonic pulses [35]. The obtained results comply with [12,14], whose authors state that increased cement contents and curing times result in higher UPV and elasticity moduli. With higher amounts of rubber, a decrease in the UPV is also apparent. As expected, the ultrasonic pulse passes through the rubber particles more slowly due to their lower density. The rubber particles have a lower specific density and a porous structure filled with air [47,48], which slows down the ultrasonic pulse.
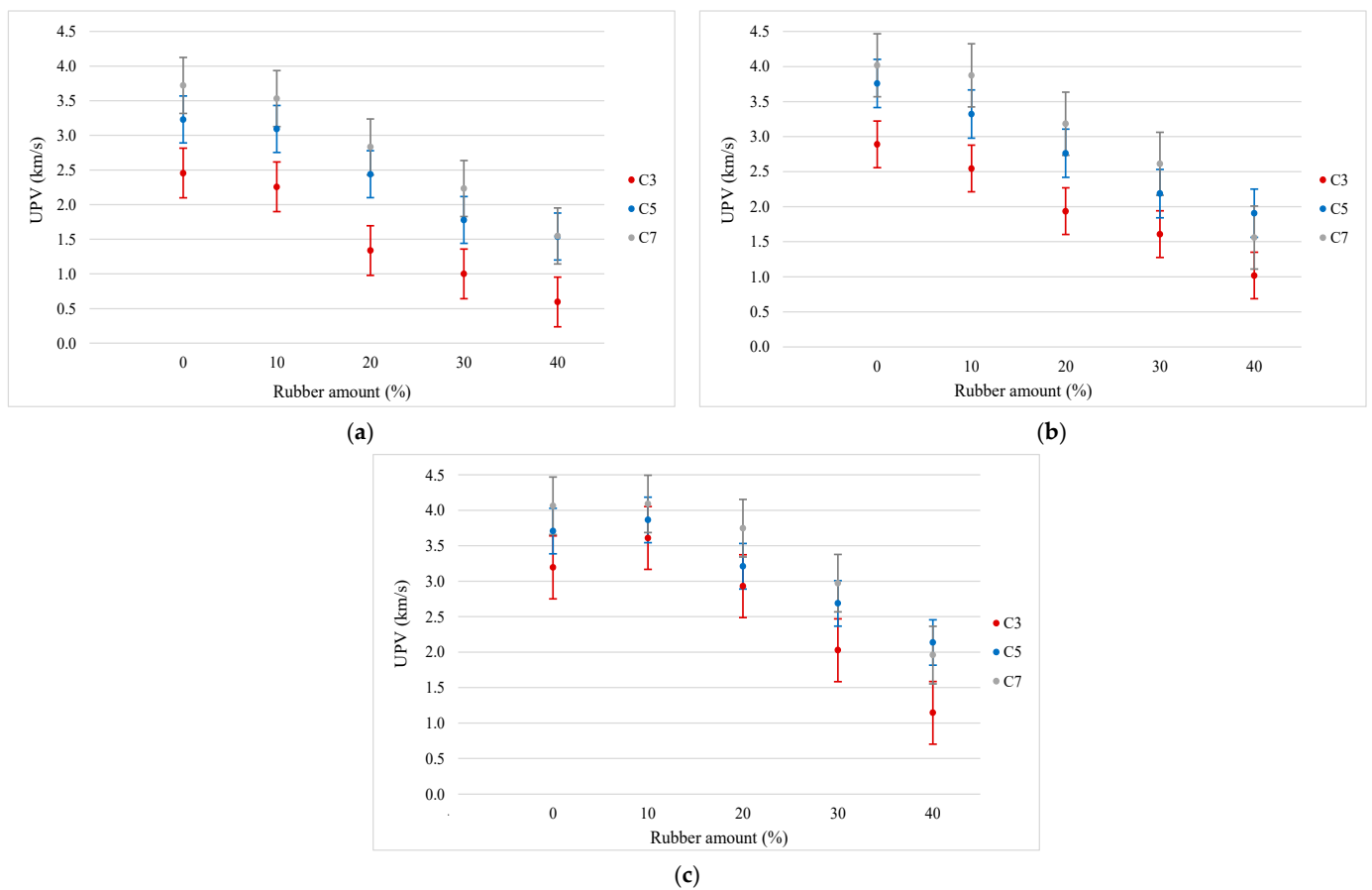
(a)

(b)

(c)

Figure 6. Impact of cement and rubber on UPV for curing periods of (**a**) 7 days, (**b**) 28 days and (**c**) 90 days.

4. Prediction Models

In order to make the results of the research conducted usable in practice, two prediction models were created by regression analysis. One was designed to predict the compressive strength (f_c) and the other was designed for the modulus of elasticity (E_{st}) prediction. In both models, the UPV was used as a predictor. This analysis was carried out based on raw pairs of data (three pairs for every mixture and curing period) of the UPV–f_c and UPV–E_{st} results. The R programming language was used to build the model. To build acceptable models, the predictors UPV and curing period were used in a linear relationship with the logarithm of the response variable.

The curing period was statistically insignificant in the model for f_c prediction based on the measured UPV values. Hence, the developed model takes only the ultrasonic pulse velocity as an input parameter. This means that the same model can be used for all three

curing periods, simplifying the prediction of f_c. The plotted data and the regression line obtained are presented in Figure 7.
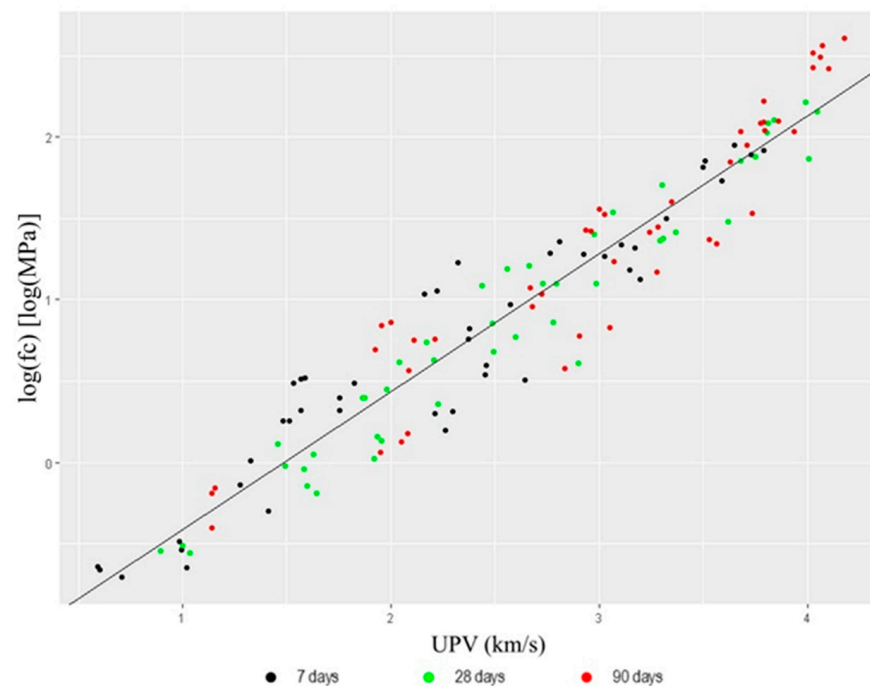

Figure 7. UPV-ln(f_c) relationship.

The model is homoscedastic (non-constant variance score test *p*-value = 0.84747), and errors are normally distributed (Shapiro–Wilk test *p*-value = 0.2124). The 95% confidence intervals for the intercept and UPV coefficient are (−1.3783653, −1.1341046) and (0.8035473, 0.8915409), respectively.

Given that this is a linear log(f_c) model, it must be transformed to obtain an expression for the prediction of f_c. The model for f_c is therefore:

$$f_c \, (\text{UPV}) = e^{(-1.25623 + 0.84754 \times \text{UPV} + \varepsilon)} = e^{\varepsilon} \times e^{(-1.25623 + 0.84754 \times \text{UPV})} \tag{1}$$

An adjusted coefficient of determination for this model equals 0.9154, which characterizes a very strong relationship. The ε is the zero mean model error, with an estimated standard deviation of 0.2414. As the hypothesis of normality was accepted, the mean prediction and prediction intervals were calculated based on the lognormal distribution, with the parameters $\mu = 0$ and $\sigma^2 = 0.2414^2 = 0.05828$. For instance, the mean prediction can be calculated by the formula:

$$\text{mean}(f_c \, (\text{UPV})) = 1.0296 \times e^{(-1.25623 + 0.84754 \times \text{UPV})} \tag{2}$$

The mean prediction line is with the 95%-prediction-interval boundaries presented in Figure 8.

The situation is more complicated in the case of E_{st} prediction based on the measured UPV values. The UPV and curing period were statistically significant, so a model with two predictors was developed. This means that the prediction of log(E_{st}) depends, apart from the UPV, on the duration of the curing period.

The model for log(E_{st}) is also homoscedastic (non-constant variance score test *p*-value = 0.38964), but the errors are not normally distributed (Shapiro–Wilk test *p*-value = 0.002291). The estimated model coefficients, intercept, UPV and days are −0.7216, 0.7585 and 0.0019, respectively, with *p*-values of 2×10^{-16}, 2×10^{-16} and 2.59×10^{-3}, respectively. Based on the asymptotic regression theory of 95% confidence intervals for

the intercept, the UPV and days coefficients are (-0.8406, -0.6025), (0.7132, 0.8038) and (0.0007, 0.0031), respectively.
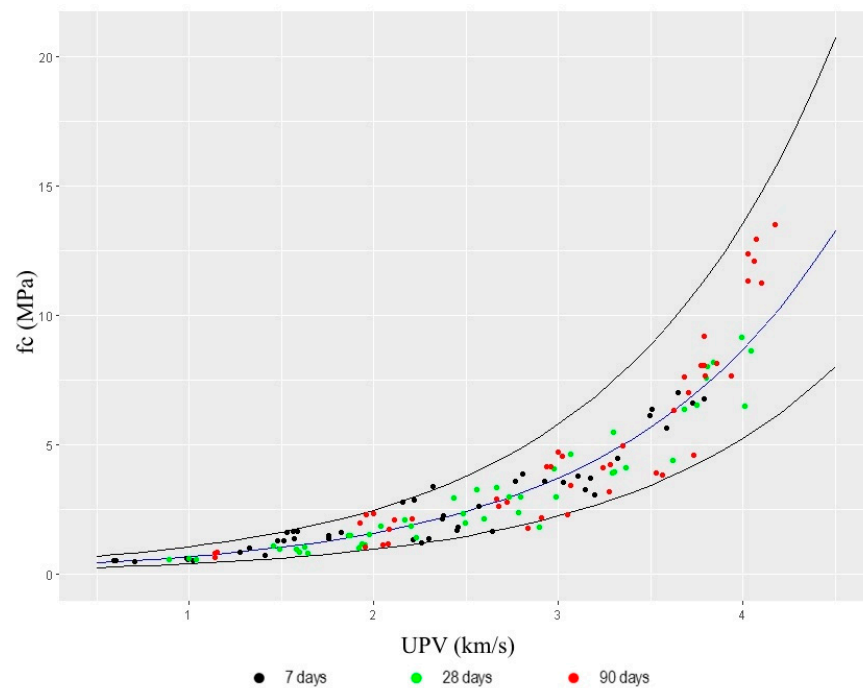

Figure 8. Mean predictions (blue line) and 2.5–97.5%-prediction-interval boundaries.

One can see that the longer curing period significantly affects the increase in E_{st}. The plotted data and the linear models obtained are presented in Figure 9. As the curing period is also a predictor, the presented lines differ for different values of the curing period.
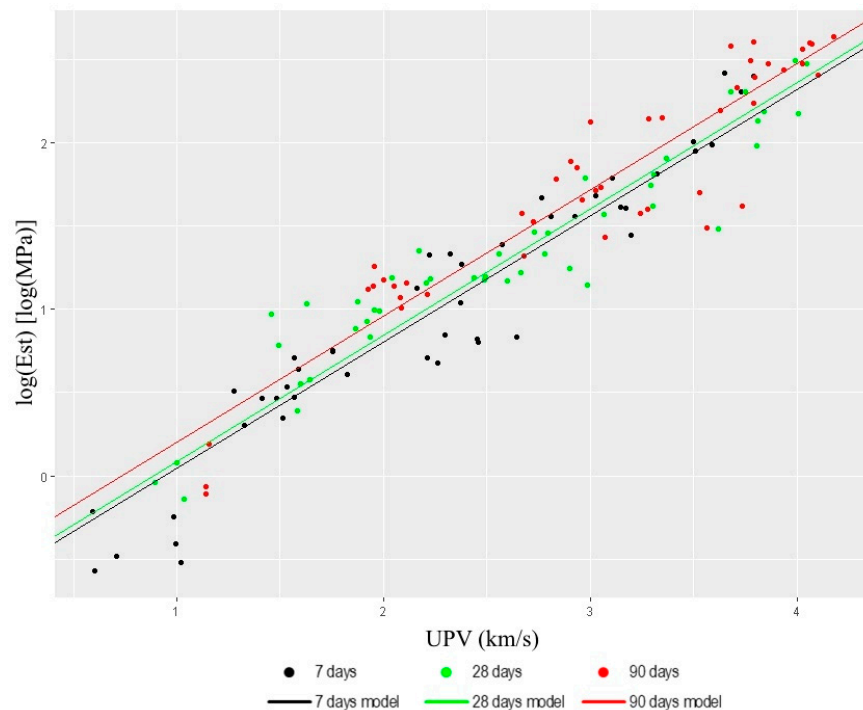

Figure 9. UPV-E_{st} relationship.

The established model is as follows:

$$E_{st}(UPV, days) = e^{-0.7216 + 0.7585 \times UPV + 0.0019 \times days + \varepsilon} = e^{\varepsilon} \times e^{-0.7216 + 0.7585 \times UPV + 0.0019 \times days} \tag{3}$$

An adjusted coefficient of determination for this model equals 0.9077, which characterizes a very strong relationship. The ε is the zero mean model error, with an estimated standard deviation of 0.2345. Extensive simulations based on the empirical error distribution showed that the e^{ε} part in the model is negligible for practical purposes, so the resulting formula can be used to discuss the behavior of the mean E_{st}, depending on UPV and days. For a complete understanding of this model, we provide the following example: for the same UPV value, a change in the curing period from 0 days to 7 days would affect an increase in E_{st} of 1.013 (GPa), a change in curing period from 0 days to 28 days would affect an increase in E_{st} of 1.055 (GPa), while changing the curing period for the same UPV from 0 to 90 days would increase E_{st} of 1.186 (GPa). The mean prediction line and 95%-prediction-interval boundaries obtained by these simulations are shown in Figure 10.
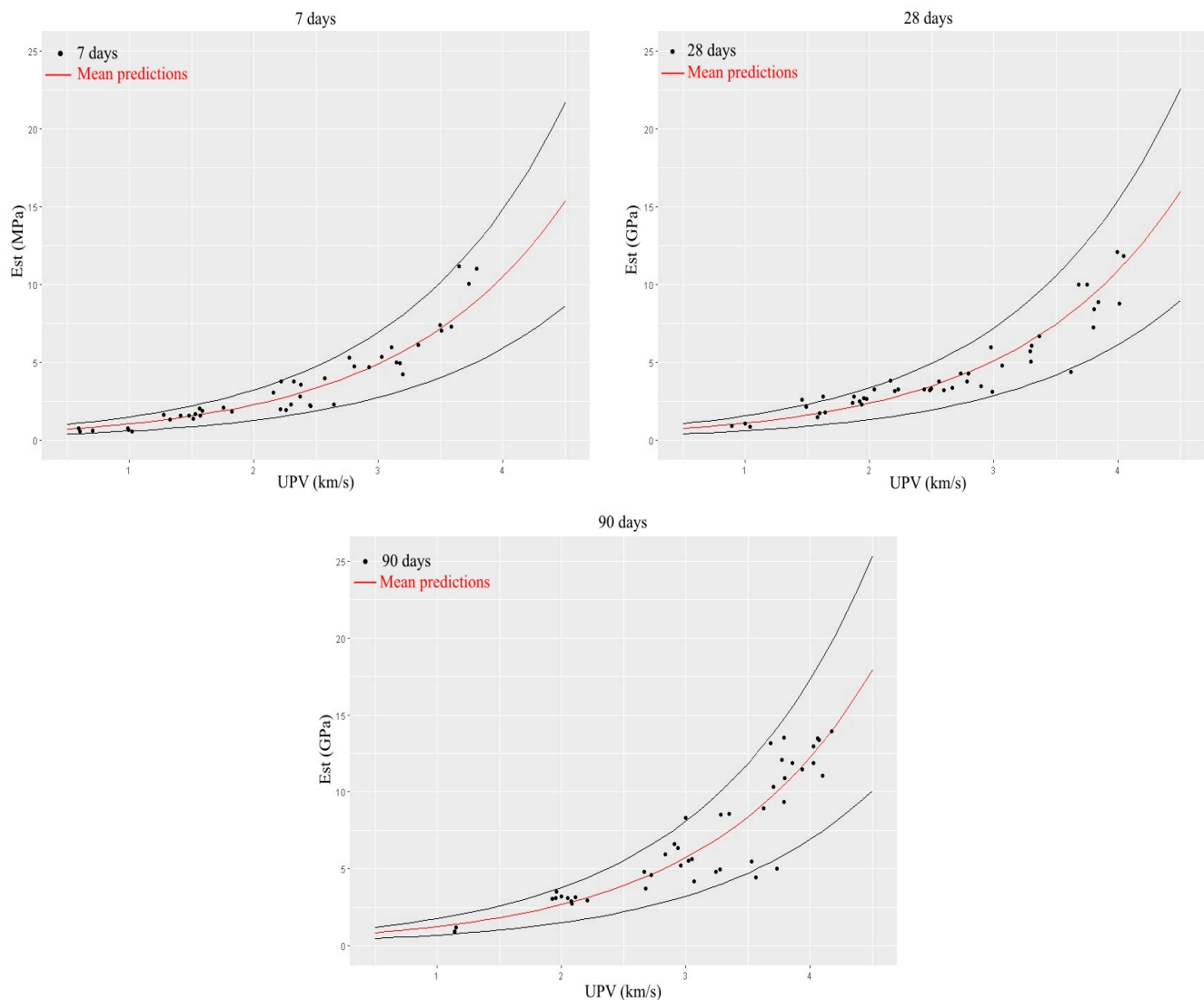

Figure 10. Mean predictions (red line) for E_{st} and 2.5–97.5%-prediction-interval boundaries.

The development of such models is significant in material testing and greatly facilitates the testing process, enabling the determination of more mechanical characteristics on the same specimen. The developed models enable reliable results, as shown by the distribution of the residuals. It was shown that the prediction of the compressive strength does not

depend significantly on the length of the curing period. In contrast, the curing period is statistically significant for predicting the static modulus of elasticity. This is in accordance with [8]. It can be concluded that, during strength development, the stiffness passes through certain phases, which cannot be determined based on the results obtained. This represents the motivation for further research and the description of the development of stiffness in cement-bound mixtures with the addition of waste rubber.

5. Conclusions

This research includes the testing of the compressive strength (f_c) and dynamic (E_{dyn}) and static (E_{st}) moduli of elasticity of cement-bound aggregate modified with waste rubber to determine the inter-relationships of these characteristics and their time dependence. Reliable results were obtained through laboratory research, enabling the development of the prediction model. These are the main contributions of this research. Furthermore, a detailed statistical analysis of nonlinear relationships, which was not found in the available research for these materials, also contributes significantly to the non-destructive testing of pavement materials. Two models were developed: one for the estimation of the f_c and the other for estimating the E_{st} based on the measured UPV and the duration of specimen curing. From the results obtained, the following conclusions can be drawn:

- Increases in the amount of cement and in the curing period positively affect the f_c, E_{dyn} and E_{st}. The addition of rubber decreases these mechanical characteristics.
- The reliability of the modulus of elasticity results obtained by the two methods is supported with a strong linear correlation ($R^2 = 0.88$).
- A detailed statistical analysis of the obtained data resulted in two simple linear prediction models. One of these models serves for the estimation of the f_c based on UPV, while the other serves for the E_{st} estimation based on the UPV and curing period.
- An inter-relationship between rubber and cement was observed, especially in the mixtures with higher proportions of cement. The recommendation for further research is to analyze this influence through more mechanical properties and on a chemical and micro level.
- The increase in the UPV in the first 7 days and its linearization for a longer period of time indicates that the CBA stiffness passes through certain phases that cannot be precisely determined from the obtained results. To determine the stage of development of the stiffness, it is recommended to carry out tests in short time intervals between the first and seventh day of care.

The presented prediction models were developed on limited data and are valid only for the tested materials. As a recommendation for further research, the verification the developed models on a more significant number of specimens and other materials is indicated to prove their general applicability. It is recommended to limit the application of these models to gravel materials, considering the shape of the grains and the manner of their entrapment.

Author Contributions: Conceptualization, M.Z. and M.B.; methodology, M.Z. and M.B.; software, M.B.; validation, M.B., I.B. and T.D.; investigation, M.Z., I.B. and T.D.; writing—original draft preparation, M.Z.; writing—review and editing, M.B., I.B. and T.D.; funding acquisition, I.B. All authors have read and agreed to the published version of the manuscript.

Institutional Review Board Statement: Not applicable.

Informed Consent Statement: Not applicable.

Data Availability Statement: Data available on request due to restrictions eg privacy or ethical. The data presented in this study are available on request from the corresponding author. The data are not publicly available due to ongoing research financed by HRZZ here].

Conflicts of Interest: The authors declare no conflicts of interest.

References

1. Zvonarić, M.; Dimter, S. Prevention and remediation measures for reflective cracks in flexible pavements. *J. Croat. Assoc. Civ. Eng.* **2022**, *74*, 189–197. [CrossRef]
2. *Development of New Bituminous Pavement Design Method*; European Commission: Brussels, Belgium, 1999.
3. Garber, S.; Rasmussen, R.O.; Harrington, D. *Guide to Cement-Based Integrated Pavement Solutions*; Portland Cement Association: Skoike, IL, USA, 2011.
4. Halsted, G.E.; Luhr, D.R.; Adaska, W.S. *Guide to Cement-Treated Base (CTB)*; Portland Cement Association: Skoike, IL, USA, 2006.
5. Marques, A.I.; Morais, J.; Morais, P.; Veiga, M.d.R.; Santos, C.; Candeias, P.; Gomes Ferreira, J. Modulus of elasticity of mortars: Static and dynamic analyses. *Constr. Build. Mater.* **2020**, *232*, 117216. [CrossRef]
6. Barišić, I.; Dokšanović, T.; Draganić, H. Characterization of hydraulically bound base materials through digital image correlation. *Constr. Build. Mater.* **2015**, *83*, 299–307. [CrossRef]
7. Jodhani, J.; Handa, A.; Gautam, A.; Ashwni Rana, R. Ultrasonic non-destructive evaluation of composites: A review. *Mater. Today Proc.* **2022**, *78*, 627–632. [CrossRef]
8. Zhao, G.; She, W.; Yang, G.; Pan, L.; Cai, D.; Jiang, J.; Hu, H. Mechanism of cement on the performance of cement stabilized aggregate for high speed railway roadbed. *Constr. Build. Mater.* **2017**, *144*, 347–356. [CrossRef]
9. Raavi, S.S.D.; Tripura, D.D. Ultrasonic pulse velocity and statistical analysis for predicting and evaluating the properties of rammed earth with natural and brick. *Constr. Build. Mater.* **2021**, *298*, 123840. [CrossRef]
10. Martin-del-Rio, J.J.; Canivelli, J. The use of non-destructive testing to evaluate the compressive strength of a lime-stabilised rammed-earth wall: Rebound index and ultrasonic pulse velocity. *Constr. Build. Mater.* **2021**, *242*, 118060. [CrossRef]
11. Zhou, T.; Zhang, H.; Li, B.; Zhang, L.; Tan, W. Evaluation of compressive strength of cement-stabilized rammed earth wall by ultrasonic-rebound combined method. *J. Build. Eng.* **2023**, *68*, 106121. [CrossRef]
12. Barišić, I.; Dimter, S.; Rukavina, T. Characterization of cement stabilized pavement layers with ultrasound testing. *Tech. Gaz.* **2016**, *23*, 447–453. [CrossRef]
13. Liu, H.; Ye, R.; Chen, L.; Ouyang, Z.; Chu, C.; Yu, H.; Lv, S.; Pan, Q. Characterization of strength, modulus, and fatigue damage properties of cement stabilized macadam based on the double modulus theory. *Constr. Build. Mater.* **2022**, *353*, 106121. [CrossRef]
14. Mandal, T.; Tinjum, J.M.; Edil, T.B. Non-destructive testing of cementitiously stabilized materials using ultrasonic pulse velocity test. *Transp. Geotech.* **2015**, *6*, 97–107. [CrossRef]
15. Mohammed, B.S.; Adamu, M.; Liew, M.S. Evaluating the effect of Crumb rubber and Nano silica on the properties of High volume fly Ash Roller compacted concrete pavement using Non-destructive Techniques. *Case Stud. Constr. Mater.* **2018**, *8*, 381–391. [CrossRef]
16. Rao, S.K.; Rao, T.C. Experimental studies in Ultrasonic Pulse Velocity of Roller compacted concrete pavement containing Fly Ash and M-sand. *Int. J. Pavement Res. Technol.* **2016**, *9*, 289–301. [CrossRef]
17. Subramanian, S.; Qasim, K.; Ku, T. Effect of sand on the stiffness characteristics of cement-stabilized clay. *Constr. Build. Mater.* **2020**, *264*, 120192. [CrossRef]
18. Norambuena-Contreras, J.; Castro-Fresno, D.; Vega Zamanillo, A.; Celaya, M.; Lombillo-Vozmediano, I. Dynamic modulus of asphalt mixture by ultrasonic direct test. *NDT E Int.* **2010**, *43*, 629–634. [CrossRef]
19. Gheibi, A.; Hedayat, A. Ultrasonic Investigation of granular materials subjected to compression and crushing. *Ultrasonics* **2018**, *87*, 112–125. [CrossRef] [PubMed]
20. Majhi, D.; Karmakar, S.; Roy, T.K. Reliability of Ultrasonic Pulse Velocity Method for Determining Dynamic Modulus of Asphalt Mixtures. *Mater. Today Proc.* **2017**, *4*, 9709–9712. [CrossRef]
21. Sarsam, S.I.; Kadium, N.S. Verifying Moisture Damage Impact in Asphalt Concrete with the Aid of Nondestructive Test NDT. *Adv. Sci. Eng.* **2020**, *12*, 13–20. [CrossRef]
22. Jackowski, M.; Małek, M. A multi-site study of a new cement composite brick with partial cement substitutes and waste materials. *Case Stud. Constr. Mater.* **2023**, *18*, e01992. [CrossRef]
23. Ramadani, S.; Abdelhamid, G.; Benmalek, M.L.; Aguiar, J.L.B. Physical and mechanical performance of concrete made with waste rubber aggregate, glass powder and silica sand powder. *J. Build. Eng.* **2019**, *21*, 302–311. [CrossRef]
24. Karalar, M.; Ozturk, H.; Özkılıç, Y.O. Experimental and numerical investigation on flexural response of reinforced rubberized concrete beams using waste tire rubber. *Steel Compos. Struct.* **2023**, *48*, 43–57. [CrossRef]
25. ETRMA. *End-of-Life Tyre. REPORT 2015*; European Tyre and Rubber Manufacturer's Association: Bruxelles, Belgium, 2015.
26. Shu, X.; Huang, B. Recycling of waste tire rubber in asphalt and portland cement concrete: An overview. *Constr. Build. Mater.* **2014**, *67 Pt B*, 217–224. [CrossRef]
27. Zeybek, Ö.; Özkılıç, Y.O.; Çelik, A.İ.; Deifalla, A.F.; Ahmad, M.; Sabri Sabri, M.M. Performance evaluation of fiber-reinforced concrete produced with steel fibers extracted from waste tire. *Front. Mater.* **2022**, *9*, 1057128. [CrossRef]
28. *EN 13286-4:2021*; Unbound and Hydraulically Bound Mixtures—Part 4: Test Methods for Laboratory Reference Density and Water Content—Vibrating Hammer. European Committee for Standardization: Brussels, Belgium, 2021.
29. *EN 933-1:1997*; Test for Geometrical Properties of Aggregates—Part 1: Determination of Particle Size Distribution—Sieving Method. European Committee for Standardization: Brussels, Belgium, 1997.

30. *EN 14227-1:2013*; Hydraulically Bound Mixtures—Specifications—Part 1: Cement Bound Granular Mixtures. European Committee for Standardization: Brussels, Belgium, 2013.
31. Zvonarić, M.; Barišić, I.; Galić, M.; Minažek, K. Influence of Laboratory Compaction Method on Compaction and Strength Characteristics of Unbound and Cement-Bound Mixtures. *Appl. Sci.* **2021**, *11*, 4750. [CrossRef]
32. Barišić, I.; Zvonarić, M.; Netinger Grubeša, I.; Šurdonja, S. Recycling waste rubber tyres in road construction. *Arch. Civ. Eng.* **2021**, *67*, 499–512. [CrossRef]
33. Farhan, A.H.; Dawson, A.; Thom, N. Behaviour of rubberised cement-bound aggregate mixtures containing different stabilisation levels under static and cyclic flexural loading. *Road Mater. Pavement Des.* **2020**, *21*, 2282–2301. [CrossRef]
34. Farhan, A.H.; Dawson, A.R.; Thom, N.H. Effect of cementation level on performance of rubberized cement-stabilized aggregate mixtures. *Mater. Des.* **2016**, *97*, 98–107. [CrossRef]
35. Farhan, A.H.; Dawson, A.R.; Thom, N.H. Compressive behaviour of rubberized cement-stabilized aggregate mixtures. *Constr. Build. Mater.* **2020**, *262*, 120038. [CrossRef]
36. Farhan, A.H.; Dawson, A.R.; Thom, N.H. Characterization of rubberized cement bound aggregate mixtures using indirect tensile testing and fractal analysis. *Constr. Build. Mater.* **2015**, *105*, 94–102. [CrossRef]
37. Farhan, A.H.; Dawson, A.R.; Thom, N.H. Recycled hybrid fiber-reinforced & cement-stabilized pavement mixtures: Tensile properties and cracking characterization. *Constr. Build. Mater.* **2018**, *179*, 488–499. [CrossRef]
38. Sun, X.; Wu, S.; Yang, J.; Yang, R. Mechanical properties and crack resistance of crumb rubber modified cement-stabilized macadam. *Constr. Build. Mater.* **2020**, *259*, 119708. [CrossRef]
39. *EN 13286-51:2004*; Unbound and Hydraulically Bound Mixtures—Part 51: Methods for the Manufacture of Test Specimens of Hydraulically Bound Mixtures Using Vibrating Hammer Compaction. European Committee for Standardization: Brussels, Belgium, 2004.
40. *CEN/TC104 TC. EN 12504-4:2021*; Testing Concrete—Part 4: Determination of Ultrasonic Pulse Velocity. European Committee for Standardization: Brussels, Belgium, 2021.
41. Barišić, I.; Dimter, S.; Rukavina, T. Cement stabilizations—Characterization of materials and design criteria. *J. Croat. Assoc. Civ. Eng.* **2011**, *63*, 8.
42. Đoković, K.; Tošović, S.; Janković, K.; Šušić, N. Physical-Mechanical Properties of Cement Stabilized RAP/Crushed Stone Aggregate Mixtures. *Tech. Gaz.* **2019**, *26*, 385–390. [CrossRef]
43. *EN 13286-43:2003*; Unbound and Hydraulically Bound Mixtures—Part 43: Test Method for the Determination of the Modulus of Elasticity of Hydraulically Bound Mixtures. European Committee for Standardization: Brussels, Belgium, 2003.
44. Barišić, I.; Dokšanović, T.; Zvonarić, M. Pavement Structure Characteristics and Behaviour Analysis with Digital Image Correlation. *Appl. Sci.* **2023**, *13*, 664. [CrossRef]
45. *EN 13286-41:2021*; Unbound and Hydraulically Bound Mixtures—Part 41: Test Method for the Determination of the Compressive Strenght of Hydraulically Bound Mixtures. European Committee for Standardization: Brussels, Belgium, 2021.
46. Rodrígues, R.S.L.; Domínguez, O.; Díaz, A.J.H.; García, C. Synergistic effects of rubber-tire-powder and fluorogypsum in cement-based composite. *Case Stud. Constr. Mater.* **2021**, *14*, e00471. [CrossRef]
47. Ul Islam, M.M.; Li, J.; Wu, Y.-F.; Roychand, R.; Saberian, M. Design and strength optimization method for the production of structural lightweight concrete: An experimental investigation for the complete replacement of conventional coarse aggregates by waste rubber particles. *Resour. Conserv. Recycl.* **2022**, *184*, 106390. [CrossRef]
48. Ul Islam, M.M.; Li, J.; Roychand, R.; Saberian, M. Investigation of durability properties for structural lightweight concrete with discarded vehicle tire rubbers: A study for the complete replacement of conventional coarse aggregates. *Constr. Build. Mater.* **2023**, *369*, 130634. [CrossRef]